

Photoacoustic Tomography of a Rat Cerebral Cortex in vivo with Au Nanocages as an Optical Contrast Agent

Xinmai Yang,[†] Sara E. Skrabalak,[‡] Zhi-Yuan Li,[§] Younan Xia,^{*,†,‡} and Lihong V. Wang^{*,†}

Department of Biomedical Engineering, Washington University in St. Louis, St. Louis, Missouri 63130, Department of Chemistry, University of Washington, Seattle, Washington 98195, and Institute of Physics, Chinese Academy of Sciences, Beijing 100080, People's Republic of China

Received September 12, 2007; Revised Manuscript Received November 4, 2007

ABSTRACT

Poly(ethylene glycol)-coated Au nanocages have been evaluated as a potential near-infrared (NIR) contrast agent for photoacoustic tomography (PAT). Previously, Au nanoshells were found to be an effective NIR contrast agent for PAT; however, Au nanocages with their more compact sizes (<50 nm compared to >100 nm for Au nanoshells) and larger optical absorption cross sections should be better suited for in vivo applications. We sequentially injected Au nanocages into the circulatory system of a rat in three administrations and in vivo PAT was conducted immediately prior to the first injection and continued until 5 h after the final injection. A gradual enhancement of the optical absorption in the cerebral cortex, by up to 81%, was observed over the course of the experiment.

Introduction. Photoacoustic tomography (PAT) is a novel, hybrid, and nonionizing imaging modality that combines the merits of both optical and ultrasonic imaging methods. It is highly sensitive to the optical absorption of biological tissue. PAT provides greater spatial resolution than purely optical imaging in deep regions while simultaneously overcoming the disadvantages of ultrasonic imaging regarding both biochemical contrast and speckle artifact; it can provide high spatial resolution images with optical contrast in a region up to 5.2 cm deep in biological tissue.^{1,2}

PAT has been successfully applied to the visualization of different structures in biological tissues and has been especially useful in imaging the cerebral cortex of small animals.^{3–7} PAT is also suitable for monitoring the circulation of exogenous optical contrast agents.^{8,9} Such contrast agents have been shown to improve the sensitivity and specificity of optical imaging techniques such as optical coherence tomography (OCT) and fluorescence imaging.¹⁰ Still, purely optical imaging techniques cannot provide high spatial

resolution in regions beyond the quasiballistic regime¹¹ (1 mm deep) because of the strong scattering in biological tissues.

Long-circulating, optically tunable nanoparticles have recently been applied to PAT as contrast agents, allowing for their uptake, delivery, and excretion from a body to be monitored. The results from such monitoring could aid in the diagnosis of cancer. For example, these small (typically 60–400 nm diameter) particles tend to extravasate and accumulate in tumor regions via a passive mechanism referred to as the enhanced permeability and retention effect,¹² which has been attributed to dysfunctional anatomical conditions such as localized leaky circulatory and lymphatic systems. This feature is especially helpful in brain tumor detection because healthy vessels in the brain dissuade the extravasation of such particles because of the blood–brain barrier. As a result, nanoparticles can accumulate in the vicinity of tumor vasculature and enhance optical contrast. In a previous study, Au nanoshells were tested as a near-infrared (NIR) optical contrast agent in PAT. In this study, we have sought to evaluate a new class of optically tunable nanoparticles, Au nanocages, as a potential contrast agent for PAT in the NIR region where the attenuation of light by blood and soft tissue is relatively low.

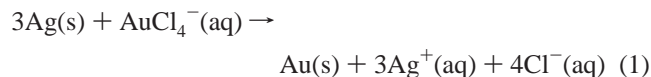
* Corresponding authors. E-mail: (Y.X. for nanocages) xia@biomed.wustl.edu; (L.V.W. for photoacoustic tomography) lhwang@biomed.wustl.edu.

[†] Washington University in St. Louis.

[‡] University of Washington.

[§] Chinese Academy of Sciences.

Gold nanocages represent a novel class of optically tunable nanoparticles.^{13–15} They are prepared by the remarkably simple galvanic replacement reaction between Ag nanocubes and HAuCl₄ as shown below^{16,17}



Owing to the template effect and reaction stoichiometry, hollow and porous Au–Ag alloyed particles, commonly referred to as Au nanocages due to its predominance, are produced. By adjusting the amount of HAuCl₄ added, the position of the localized surface plasmon resonance (LSPR) peaks of the resultant Au nanocages can be precisely tuned throughout the visible and into the NIR region. Owing to the biocompatibility and well-established surface chemistry of Au, we have started to explore the optical properties of Au nanocages for a number of biomedical applications.^{18,19} For example, it has recently been demonstrated that Au nanocages provide enhanced image contrast when integrated with OCT, an imaging modality capable of resolving tissue microanatomy *in vivo* using predominantly scattering contrast.^{20,21} Additionally, Au nanocages functionalized with targeting moieties have been shown to preferentially accumulate on the surface of cancer cells.²¹ The subsequent absorption of NIR light by the immuno-targeted Au nanocages resulted in the selective photothermal destruction of cancer cells *in vitro*.²²

This work aims to tailor the optical properties of the Au nanocages for use with PAT. To this end, we have prepared Au nanocages with an average edge length of ~50 nm. Discrete dipole approximation (DDA) calculations indicate that these small, hollow Au nanostructures have a particularly large optical absorption cross section, nearly 5 orders of magnitude greater than that of conventional organic dyes.²³ This feature is attractive to absorption-based imaging techniques such as PAT. Specifically, we show the feasibility of Au nanocages as an intravascular contrast agent for PAT of small animals *in vivo*. The vasculature of a rat's cerebral cortex was imaged, and an enhanced optical contrast was observed with the use of Au nanocages.

Methods. Au nanocages with an edge length of ~50 nm were prepared in a two-step process. First, Ag nanocubes (Figure 1A) were prepared by a rapid, sulfide-mediated polyol process in which Ag(I) is reduced to Ag(0) in the presence of ethylene glycol, poly(vinyl pyrrolidone), and a trace amount of sodium sulfide.²⁴ The isolated Ag nanocubes were converted into Au nanocages (Figure 1B) via the galvanic replacement reaction. To a heated suspension of Ag nanocubes, HAuCl₄ solution was added until the reaction media appeared dark blue, indicating a red-shift of the SPR. The resulting Au nanocages had a peak optical absorption at ~820 nm (Figure 1C), a wavelength that overlaps with the optical extinction window of biological tissues. The nanocage surfaces were then functionalized with poly(ethylene glycol) (PEG, MW = 5000), which has been shown to suppress immunogenic responses and thus increase the blood circulation time.^{25,26}

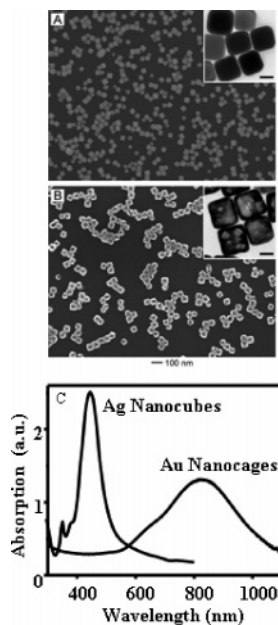


Figure 1. (A) SEM image of the as-synthesized silver nanocubes with edge lengths of ~40 nm. (B) SEM image of gold nanocages (edge length of ~50 nm) prepared by the galvanic replacement reaction between Ag nanocubes and HAuCl₄ solution. (C) Absorption spectra of Ag nanocubes and Au nanocages. The insets in panels A and B show TEM images of the nanocubes and nanocages, respectively (scale bars: 25 nm).

The setup for noninvasive PAT of rat brains is similar to that in the previous work⁸ and has been described in detail in the Supporting Information. In the *in vivo* test, Au nanocages were injected into the circulatory system of a rat through the tail or saphenous vein. Similar to the previous work,⁸ three successive injections of nanocages were administered, each with a dose of $\sim 0.8 \times 10^9$ nanocages/g body weight. PAT scanning started immediately following each administration. After three administrations, PAT scanning was continuously performed for over 5 h. With another animal, a single injection with a dose of $\sim 0.8 \times 10^9$ nanocages/g body weight was also performed, and PAT scanning immediately followed the injection and continued for about 3 h. The laser wavelength used was 804 nm. In every *in vivo* experiment, after data acquisition the rat was sacrificed with an overdose injection of pentobarbital. Open skull surgery was performed to photograph the cerebral cortex.

To further understand the contrast enhancement, we measured the photoacoustic signal generated by Au nanocages mixed with rat blood *ex vivo* while a single dose of $\sim 0.8 \times 10^9$ nanocages/g body weight was used. First, nanocages were mixed with rat blood at a ratio equivalent to $\sim 0.8 \times 10^9$ nanocages/g body weight and injected into a small Tygon tube (940 μm OD, 510 μm ID). The tube was then illuminated by the laser while the generated photoacoustic signals were detected by an ultrasonic transducer. The laser wavelength was tuned from 764 to 824 nm, and the photoacoustic signals were collected at different wavelengths. As a reference, the photoacoustic signals generated by pure rat blood were also measured.

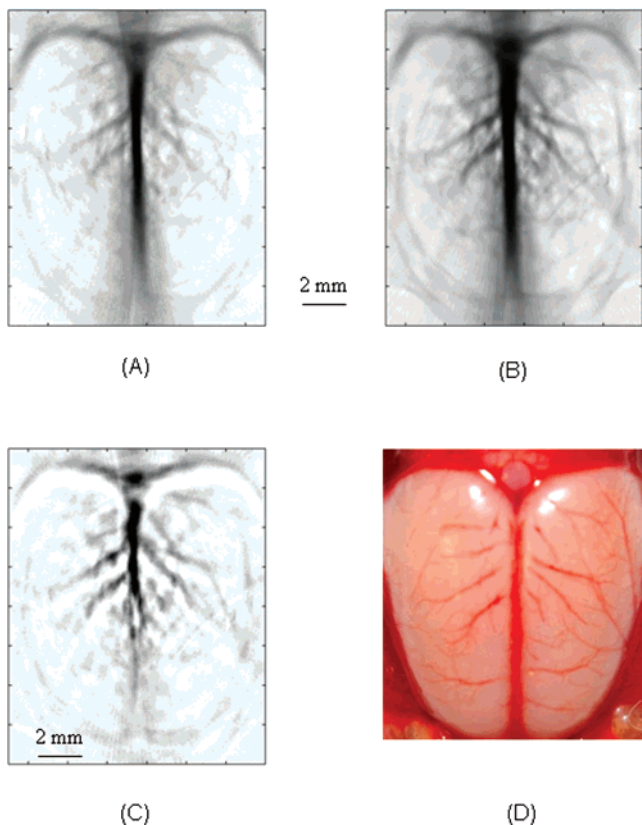


Figure 2. Noninvasive PAT imaging of a rat's cerebral cortex (A) before the injection of nanocages and (B) about 2 h after the final injection of nanocages, which is the peak enhancement point. (C) A pixelwise differential image (image B–image A). (D) An open-skull photograph of the rat's cerebral cortex. Three successive injections were administered in these results.

Results and Discussion. PAT images of the cerebral cortex of a rat of the three successive injections are presented in Figure 2. Figure 2A,B were taken before and after the injection of Au nanocages, respectively. Compared with Figure 2A, which only shows the intrinsic optical contrast, Figure 2B reveals the brain vasculature with greater clarity. This enhanced clarity was due to the injected Au nanocages. With Au nanocages, the optical absorption of the blood was increased and hence the contrast between blood in vessels and the background brain tissues was enhanced. A differential image shown in Figure 2C was obtained by subtracting pixelwise the amplitude of the preinjection image (Figure 2A) from that of the postinjection image (Figure 2B). This image displays the distribution of differential optical absorption in the rat brain as induced by Au nanocages. All the PAT images of the rat brain match well with the open-skull anatomical photograph in Figure 2D.

The increases in optical absorption after nanocage injection were calculated for all PAT images. The signals were integrated over each image and then normalized to the signal integration of the reference image. The results are shown in Figure 3. The enhancements in the blood absorption have a peak value of 81%, which occurs about 2 h after the final injection. This enhancement is comparable but greater than the previously reported 63% enhancement when Au nanoshells were used as a contrast agent at a similar dose.⁸ After the

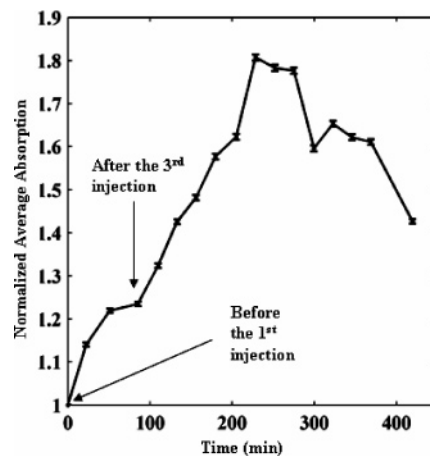


Figure 3. The integrated absorption calculated from the experimental images for the three-successive-injection experiment. The presented values are normalized by the integrated absorption of the image obtained before the injection. The error bars are the standard errors for each integration.

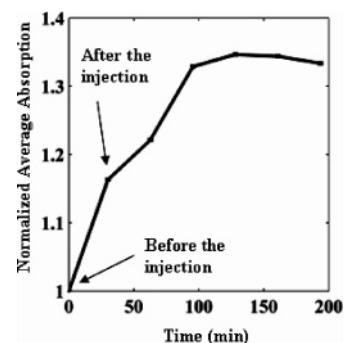


Figure 4. The integrated absorption calculated from the experimental images for the single-injection experiment. The presented values are normalized by the integrated absorption of the image obtained before the injection. The error bars are the standard errors for each integration.

maximum enhancement was achieved, the absorption gradually decreased, presumably due to clearance of the nanocages from the blood.²⁷

Figure 4 shows the enhancement result for a single injection, whereas Figure 5 shows the ex vivo results. In Figure 4, the enhancements have a peak value of 35%, which occurs about 2 h after the injection. Figure 5 shows the measured photoacoustic signal amplitude generated by Au nanocages in rat blood at several wavelengths. With blood only, the amplitudes of measured photoacoustic signals are considerably lower. After adding the Au nanocages into the blood, the amplitudes increase by 85–106% over this wavelength range.

According to Figure 5, the blood absorption should be improved by 95% at a single injection of $\sim 0.8 \times 10^9$ ex vitro, but we observed only a 35% enhancement in vivo in Figure 4. In the previous work with Au nanoshells,⁸ $\sim 30\%$ enhancement in absorption was reported in vivo while $\sim 100\%$ enhancement was expected according to the calculation, which is probably due to biological effects.

In both Figures 3 and 4, the results showed the peak enhancement came about 2 h after the injection (or the final

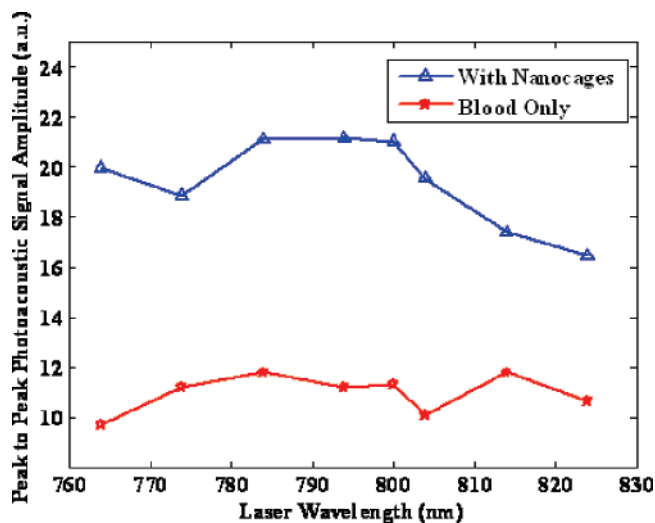


Figure 5. Ex vivo measurements of optical absorption spectral of rat blood with and without Au nanocages.

injection in Figure 3). The delay may relate to the circulation mechanism of these nanoparticles in the blood stream, which is being studied independent of this study.

To further compare Au nanoshells and Au nanocages, we simulated the extinction spectra for both nanoparticles in water. The parameters used in the simulations were 145 nm outer diameter and 125 nm inner diameter with a shell thickness of 10 nm for the Au nanoshells and 50 nm outer edge and 42 nm inner edge with a wall thickness of 4 nm for the Au nanocages (alloy composition 70% Au and 30% Ag). Mie theory and DDA were employed for the calculation of nanoshell and nanocage particles, respectively. These dimensions are similar to those materials used in the previous⁸ and current work. The calculation results are shown in Figure 6. Overall, Au nanoshells have a much greater extinction value than Au nanocages. However, the extinction of Au nanoshells is dominated by scattering. In contrast, the extinction of Au nanocages is dominated by absorption. Around 800 nm, Au nanocages have a greater absorption cross-section than Au nanoshells (0.036 versus 0.027 μm^2). Since PAT is an absorption-based technique, the greater absorption of the Au nanocages makes them more suitable than Au nanoshells for use as a contrast agent, as demonstrated in this study.

Conclusion. We have demonstrated that Au nanocages can be used in PAT to enhance the contrast between blood and the surrounding tissues. The enhanced contrast could allow more detailed vascular structures to be imaged at greater depths. Our results indicate that Au nanocages are promising contrast agents for imaging techniques based on optical absorption and in particular for PAT. Compared with Au nanoshells, Au nanocages seem to have slight advantages in PAT due to their absorption-dominant extinction. In addition, it may also benefit thermal therapy based on these nanoparticles. The smaller sizes of nanocages should be advantageous for in vivo delivery. We envision that PAT with Au nanocages bioconjugated to target cancer cells could provide a powerful tool for cancer detection.

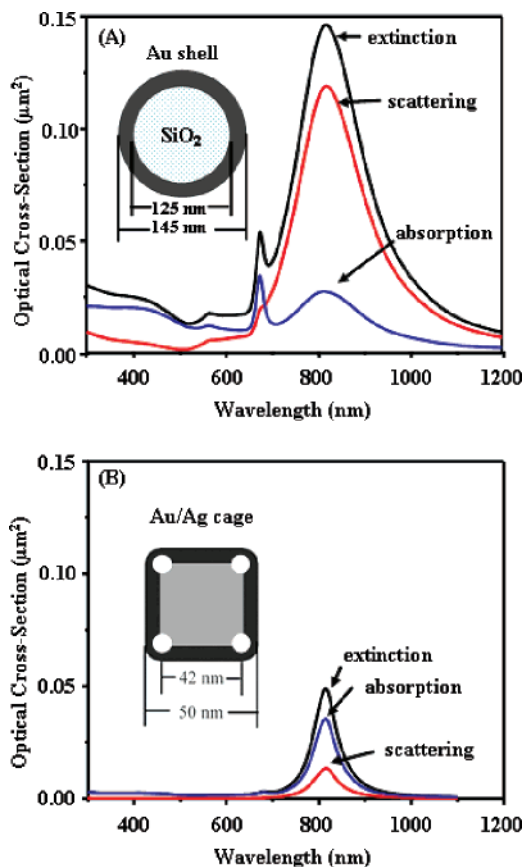


Figure 6. Extinction spectra calculated using Mie theory and the DDA method for (A) a Au nanoshell composed of a SiO_2 core (diameter = 125 nm) and 10 nm thick Au shell and (B) a Au nanocage with an edge length of 50 nm and wall thickness of 4 nm, respectively. Both were simulated to be in a water environment.

Acknowledgment. We thank Erich Stein for experimental assistance. This project was supported in part by the National Institutes of Health (NIH) Grants R01 NS46214 and R01 EB000712 (both to L.V.W.), as well as an NIH Director's Pioneer Award (5DP1OD000798) and a National Science Foundation Grant (DMR-0451788) (both to Y.X.). Z.Y.L. thanks the National Natural Science Foundation of China (Nos. 10525419 and 60736041) for financial support.

Supporting Information Available: Experimental details including Au nanocage preparation, PAT experimental setup, and schematic of PAT of the rat brain in vivo. This material is available free of charge via the Internet at <http://pubs.acs.org>.

References

- (1) Ku, G.; Wang, L. V. *Opt. Lett.* **2005**, *30*, 507–509.
- (2) Ku, G.; Fornage, B. D.; Jin, X.; Xu, M.; Hunt, K. K.; Wang, L. V. *Technol. Cancer Res. Treat.* **2005**, *4*, 559–566.
- (3) Wang, X.; Pang, Y.; Ku, G.; Xie, X.; Stoica, G.; Wang, L. V. *Nat. Biotechnol.* **2003**, *21*, 803–806.
- (4) Hoelen, C. G. A.; de Mul, F. F. M.; Pongers, R.; Dekker, A. *Opt. Lett.* **1998**, *23*, 648–650.
- (5) Kruger, R. A.; Reinecke, D. R.; Kruger, G. A. *Med. Phys.* **1999**, *26*, 1832–1837.
- (6) Oraevsky, A. A.; Wang, L. V. *Proc. SPIE* **2006**, 6086.
- (7) Xu, M.; Wang, L. V. *Rev. Sci. Instrum.* **2006**, *77*, 041101, 1–22.
- (8) Wang, Y.; Xie, X.; Wang, X.; Ku, G.; Gill, K. L.; O'Neal, D. P.; Stoica, G.; Wang, L. V. *Nano Lett.* **2004**, *4*, 1689–1692.

- (9) Wang, X.; Ku, G.; Wegiel, M. A.; Bornhop, D. J.; Stoica, G.; Wang, L. V. *Opt. Lett.* **2004**, *29*, 730–732.
- (10) Licha, K. In *Topics in Current Chemistry*; Springer: Berlin/Heidelberg, 2002; pp 1–29.
- (11) Wang, L. V.; Wu, H.-i. *Biomedical Optics: Principles and Imaging*; Wiley: New York, 2007.
- (12) Maeda, H. *Adv. Drug Delivery Rev.* **1991**, *6*, 181–202.
- (13) Sun, Y.; Xia, Y. *Science* **2002**, *298*, 2176–2179.
- (14) El-Sayed, M. A. *Acc. Chem. Res.* **2001**, *34*, 257–264.
- (15) Ramachandra Rao, C. N.; Kulkarni, G. U.; Thomas, P. J.; Edwards, P. P. *Chem. Soc. Rev.* **2000**, *29*, 27–35.
- (16) Sun, Y.; Mayers, B.; Xia, Y. *Nano Lett.* **2002**, *2*, 481–485.
- (17) Sun, Y.; Xia, Y. *J. Am. Chem. Soc.* **2004**, *126*, 3892–3901.
- (18) Skrabalak, S. E.; Chen, J.; Au, L.; Lu, X.; Li, X.; Xia, Y. *Adv. Mater.* **2007**, in press.
- (19) Hu, M.; Chen, J.; Li, Z.-Y.; Au, L.; Hartland, G. V.; Li, X.; Marquez, M.; Xia, Y. *Chem. Soc. Rev.* **2006**, *35*, 1084–1094.
- (20) Cang, H.; Sun, T.; Li, Z.-Y.; Chen, J.; Wiley, B. J.; Xia, Y.; Li, X. *Opt. Lett.* **2005**, *30*, 3048–3050.
- (21) Chen, J.; Saeki, F.; Wiley, B. J.; Cang, H.; Cobb, M. J.; Li, Z.-Y.; Au, L.; Zhang, H.; Kimmey, M. B.; Li, X.; Xia, Y. *Nano Lett.* **2005**, *5*, 473–477.
- (22) Chen, J.; Wang, D.; Xi, J.; Au, L.; Siekkinen, A.; Warsen, A.; Li, Z.-Y.; Zhang, H.; Xia, Y.; Li, X. *Nano Lett.* **2007**, *7*, 1318–1322.
- (23) Chen, J.; Wiley, B.; Li, Z.-Y.; Campbell, D.; Saeki, F.; Cang, H.; Au, L.; Lee, J.; Li, X.; Xia, Y. *Adv. Mater.* **2005**, *17*, 2255–2261.
- (24) Siekkinen, A. R.; McLellan, J. M.; Chen, J. Y.; Xia, Y. *Chem. Phys. Lett.* **2006**, *432*, 491–496.
- (25) Chen, A. M.; Scott, M. D. *BioDrugs* **2001**, *15*, 833–847.
- (26) Harris, J. M.; Martin, N. E.; Modi, M. *Clin. Pharmacokinet.* **2001**, *40*, 539–551.
- (27) James, W. D.; Hirsch, L. R.; West, J. L.; O’Neal, P. D.; Payne, J. D. *J. Radioanal. Nucl. Chem.* **2007**, *271*, 455–459.

NL072349R